WANL-PR(Q)-009

NASA-CR-54935

GPO PRICE $ ______

CFSTI PRICE(S) $ ______

Hard copy (HC) 2.00

Microfiche (MF) .50

ff 653 July 65

DEVELOPMENT OF DISPERSION STRENGTHENED TANTALUM BASE ALLOY

Eighth Quarterly Report

by

R.W. Buckman and R.C. Goodspeed

prepared for

National Aeronautics and Space Administration

Lewis Research Center

Space Power Systems Division

Under Contract (NAS 3-2542)

N66 26863

(ACCESSION NUMBER)

42

(PAGES)

NASA-CR-54935

(NASA CR OR TMX OR AD NUMBER)

(THRU)

1

(CODE)

17

(CATEGORY)

FACILITY FORM 602

Astronuclear Laboratory

Westinghouse Electric Corporation

NOTICE

Copies of this report can be obtained from:

National Aeronautics & Space Administration
Office of Scientific and Technical Information
Washington 25, D. C.
Attention: AFSS-A

Astronuclear Laboratory

WANL-PR-(Q)-009
NASA-CR-54935

DEVELOPMENT OF DISPERSION STRENGTHENED TANTALUM BASE ALLOY

by

R. W. Buckman, Jr.

and

R. C. Goodspeed

EIGHTH QUARTERLY PROGRESS REPORT

Covering the Period

August 20, 1965 to November 20, 1965

Prepared For

NATIONAL AERONAUTICS AND SPACE ADMINISTRATION
Contract NAS 3-2542

Technical Management
Paul E. Moorhead
NASA-Lewis Research Center
Space Power Systems Division

Astronuclear Laboratory
Westinghouse Electric Corporation
Pittsburgh 36, Pa.

Astronuclear Laboratory

ABSTRACT

26863

Development of dispersion strengthened tantalum base alloys for use in advanced space power systems continued with the processing of the side forged ingot of composition NASV-20 (Ta-8W-1Re-0.7Hf-0.025C) to sheet. Evaluation of this material is presently underway. Further phase identification and morphology work was performed, using optical and electron microscopy and x-ray and electron diffraction techniques.

TABLE OF CONTENTS

LIST OF FIGURES

LIST OF TABLES

I. INTRODUCTION

This, the Eighth Quarterly Progress Report on the NASA-sponsored program, "Development of a Dispersion Strengthened Tantalum Base Alloy", describes the work accomplished during the period August 20, 1965 to November 20, 1965. The work was performed under Contract NAS 3-2542.

The primary objective of this Phase II work is the double vacuum arc melting of three compositions in the form of 60-pound, 4-inch diameter ingots. These compositions are to be used for sheet and tubing applications and will be selected for their weldability, creep resistance, and fabricability characteristics.

Prior to this quarterly period several promising tantalum alloy compositions were developed.[1] These alloys exhibited good creep resistance to at least 1315°C (2400°F) while maintaining adequate fabricability and weldability. From these alloys a weldable composition containing a carbide dispersion, NASV-20 (Ta-8W-1Re-0.7Hf-0.025C), was selected and melted as the first 4-inch diameter ingot. The bottom section of the NASV-20 ingot was upset forged and processed to 0.04-inch sheet. Evaluation of this sheet was initiated. A second section of the NASV-20 ingot was side forged. Seven additional 2-inch diameter ingot compositions were selected, processed, and evaluated to further optimize the carbo-nitride dispersion strengthened compositions with respect to fabricability, weldability, thermal stability, and creep strength before selection of the remaining two 4-inch diameter ingot compositions. Phase identification and morphology studies were initiated on NASV-20 and continued on other tantalum alloy compositions containing carbo-nitride dispersoids.

During this quarterly period the NASV-20 side forging was processed to 0.04-inch sheet. Evaluation of this sheet was initiated and evaluation of sheet previously processed from the upset forging continued. Detailed processing information, including dimensions, weights, hardnesses, grain sizes, and microstructures for composition NASV-20 was compiled. Phase identification and morphology studies were continued on NASV-20.

II. PROGRAM STATUS

A. FOUR-INCH DIAMETER INGOT SCALE-UP

Secondary Working — The 24.6-pound conditioned side forged billet of NASV-20 was annealed for 2 hours at 1480°C (2700°F) and rolled from a thickness of 1-1/8 inch to a thickness of 1/4 inch at 500°C (930°F) by Fansteel Metallurgical Corporation. The resulting excellent quality plate was about 26 inches long x 6-1/2 inches wide (Figure 1). This plate was then sectioned into three pieces which, when conditioned were 6.4 inches x 18 inches weighing 17.3 pounds, 5 inches x 3.4 inches weighing 2.6 pounds, and 3 inches x 4.5 inches weighing 2.1 pounds. The two smaller pieces were processed by the standard process to 0.04-inch sheet. Evaluation of this sheet for weldability, mechanical properties, and creep resistance is in progress. The largest piece of plate will be processed to an 18 inch wide x 36 inch long x 0.04 inch thick sheet.

The complete processing schedule for composition NASV-20 from the as-cast ingot to 0.04 inch sheet is shown in Figure 2. Also included are the dimensions, weights, hardnesses, and grain sizes (standard line intercept method) at the various stages of processing. The microstructure of the as-cast material is shown in Figure 3 and the microstructure of the material after the various stages of processing is shown in Figures 4 and 5.

Weldability — Tungsten inert gas (TIG) bead-on-plate welds were made on 0.040-inch NASV-20 sheet which was processed from the side forging. The sheet was annealed for 1 hour at 1650°C (3000°F) prior to welding. The ductile-brittle transition temperature (DBTT) of the as-TIG welded material and of the base metal were determined. These results, along with the results previously obtained on NASV-20 sheet processed from the upset forging are recorded in Table 1. A DBTT of <-320°F for the base metal and of -150 to -250°F for the as-TIG welded material is indicative of the good intrinsic ductility of NASV-20.

Mechanical Property Evaluation — Tensile data were obtained at -320, -150, 70, and 600°F (-195, -101, 21, and 315°C) on 0.040-inch thick sheet specimens which had been

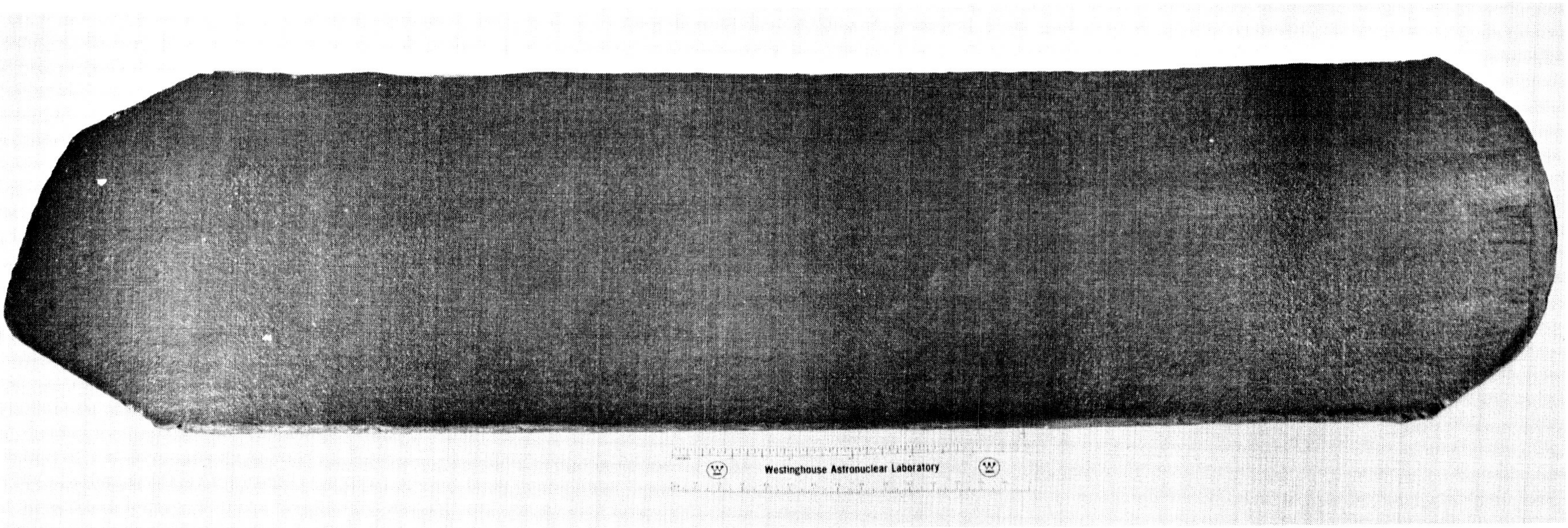

FIGURE 1 - Quarter Inch Thick Plate of NASV-20 (Ta-8W-1Re-0.7Hf-0.025C) Processed from Side Forging.

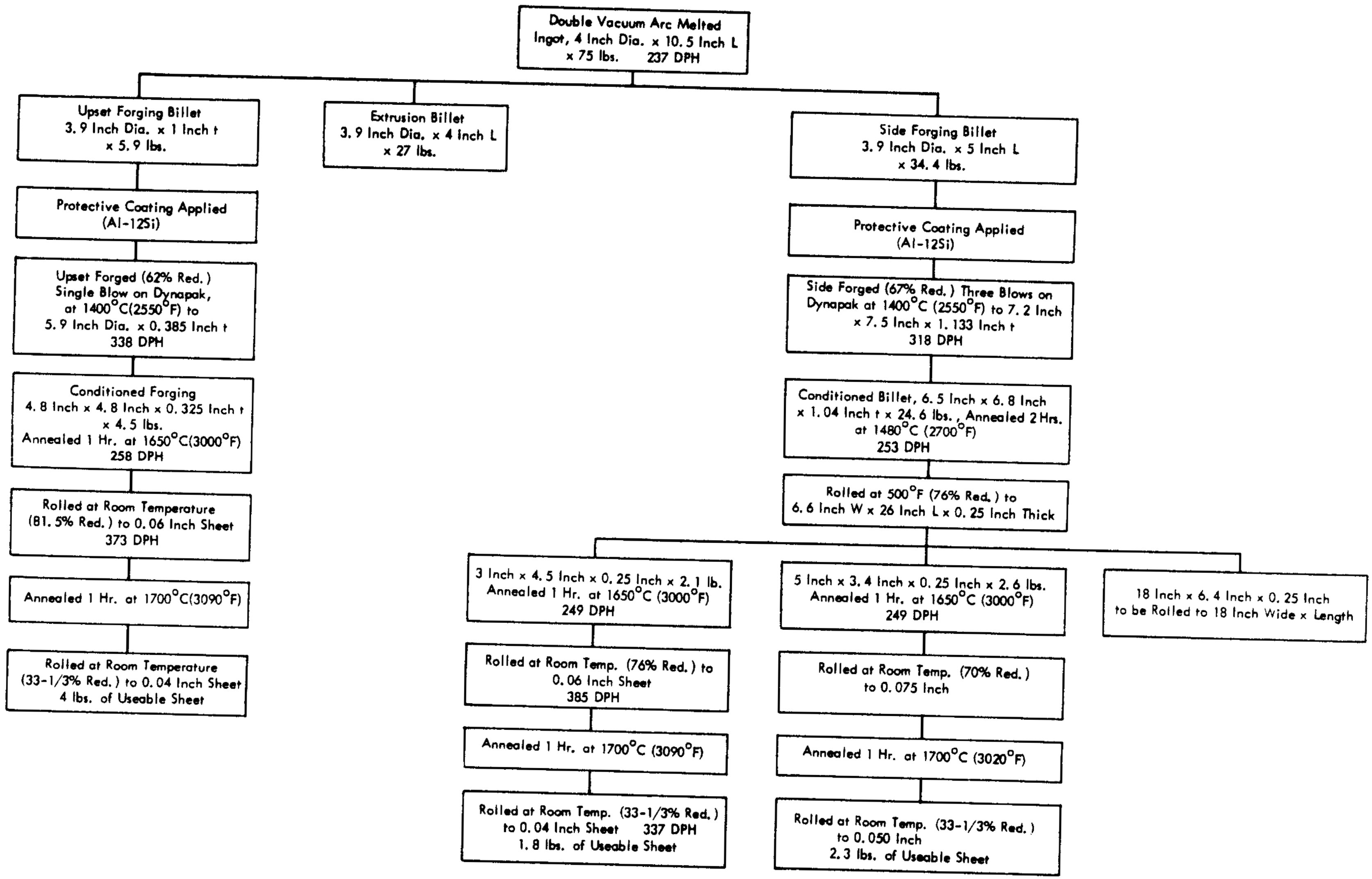

FIGURE 2 - Schedule for Processing NASV-20

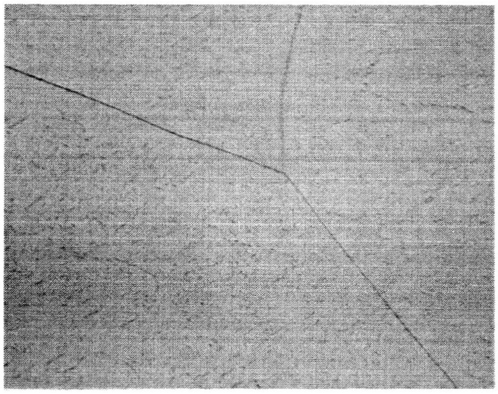

a. 150x

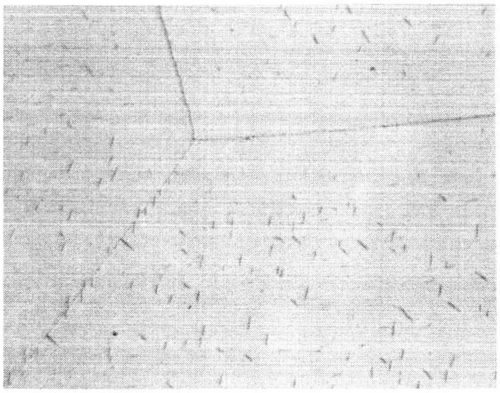

b. 500x

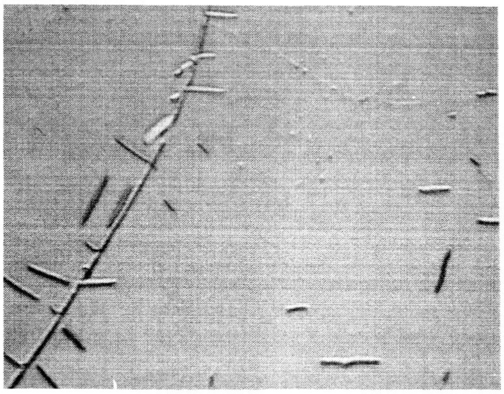

c. 1500x

FIGURE 3 - Microstructure of As-Cast NASV-20 (Ta-8W-1Re-0.7Hf-0.025C)
(Etchant - 1 part HNO_3, 1 part HF, 2 parts glycerine)
Oblique Light

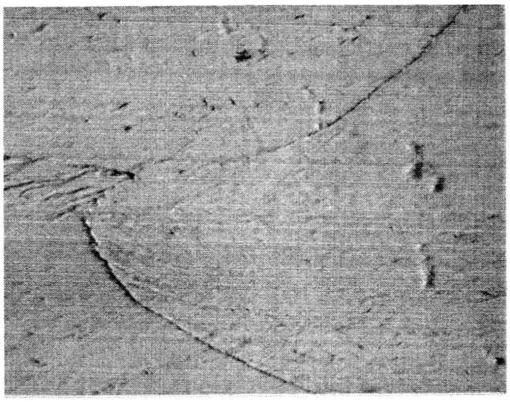

a. Upset Forged
338 DPH

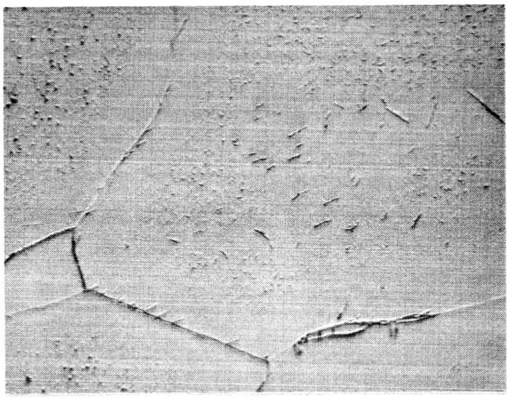

b. Upset Forged and
Annealed for 1 Hr.
at 1650°C(3000°F)
258 DPH

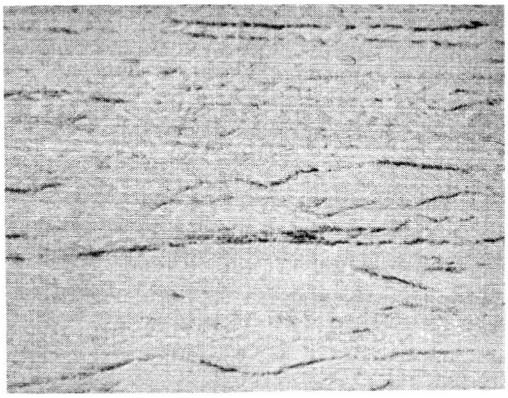

c. As-Rolled (0.06"
Sheet)
373 DPH

FIGURE 4 - Microstructure of NASV-20 (Ta-8W-1Re-0.7Hf-0.025C) at Various Stages of Processing Upset Forging to Sheet (500x)
(Etchant - 1 part HNO_3, 1 part HF, 2 parts glycerine)

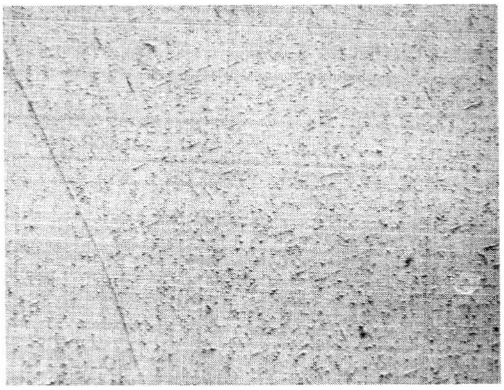

a. Side Forged 318 DPH

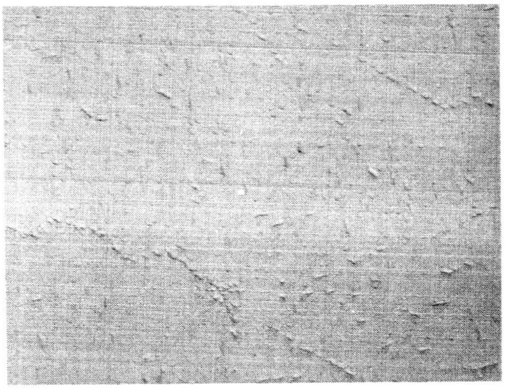

b. Side Forged and Annealed for 2 Hrs. at 1480°C(2700°F) 253 DPH

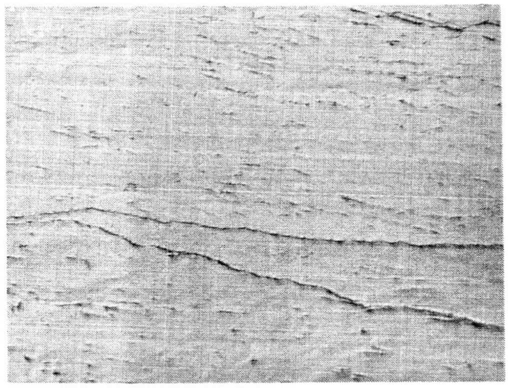

c. As-Rolled(1/4" Plate) 365 DPH

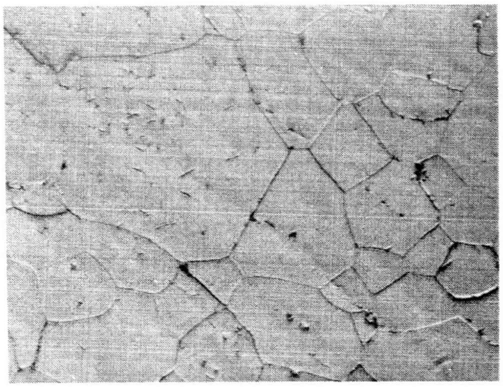

d. As-Annealed for 1 Hr. at 1650°C (3000°F) (1/4" Plate) 249 DPH

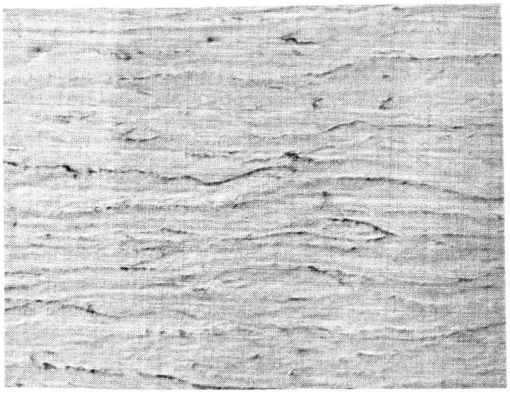

e. As-Rolled(0.06" Sheet) 385 DPH

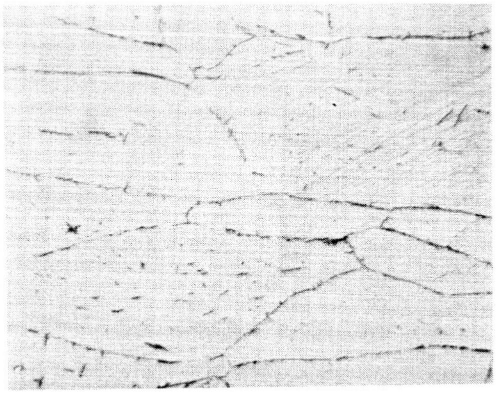

f. As-Rolled(0.04" Sheet) 337 DPH

FIGURE 5 - Microstructure of NASV-20 (Ta-8W-1Re-0.7Hf-0.025C) at Various Stages of Processing Side Forging to Sheet (500x)
(Etchant - 1 part HNO_3, 1 part HF, 2 parts glycerine)

TABLE 1 - Ductile-Brittle Transition Temperature of Composition NASV-20[a] (Ta-8W-1Re-0.7Hf-0.025C)

Condition	Test Temperature °F	°C	No Load Bend Angles (Degrees)	Remarks	DBTT (°C/°F)
Base Metal					
(Side Forging)	-320	-195	96	Bend	<-195/-320
(Upset Forging)	-320	-195	96	Bend	<-195/-320
Electron Beam					
(Upset Forging)	-320	-195	96	Bend	<-195/-320
TIG Welded					
(Side Forging)	-150	-101	95	Bend[b]	-101/-150
	-200	-129	60	Break	
(Upset Forging)	-250	-151	95	Bend	<-157/-250

(a) 0.040-inch sheet annealed for 1 hour at 1650°C/3000°F prior to welding and/or testing. Bend radius of 1.8t used.

(b) Sample exhibited slight ductile failure.

processed from the NASV-20 side forging. Prior to testing, each specimen was annealed for 1 hour at 1650°C (3000°F). The data are recorded in Table 2 and plotted in Figure 6. Also reported are data on NASV-20 sheet processed from the upset forging. The properties of this sheet are identical to the properties of the sheet from the side forged billet. As previously stated,[2] NASV-20's yield strength, ultimate tensile strength, and tensile elongation are all intermediate to those of T-111 and T-222 over the temperature range of room temperature to about 1650°C (3000°F).

Testing of five more specimens at temperatures of 1500, 2000, 2200, 2600, and 2800°F (816, 1093, 1205, 1427, and 1538°C) has been delayed by a breakdown of instrumentation. These tests will be completed during the next report period.

<u>Creep Properties</u> — Creep testing of NASV-20 sheet will be initiated during the next reporting period. During this period, the ultra-high vacuum creep testing equipment was relocated, interrupting testing for approximately 4 weeks. After the equipment relocation was completed, the remaining specimens from the optimization investigation were completed. This data will be discussed in a latter section of this report.

<u>Phase Identification and Morphology</u> — Phase identification and morphology studies were continued on composition NASV-20. Standard Debye-Scherrer x-ray diffraction analyses were made on residues chemically extracted[3,4] from NASV-20 in the cast, upset forged, side forged and sheet conditions. Besides some undissolved BCC tantalum, the only phase present in any of the residues was the HCP tantalum dimetal carbide. The back reflection diffraction lines were too broad and diffuse to accurately determine the lattice parameters a_o and c_o. However, they were in the general range of 3.10 to 3.12 Å and 4.92 to 4.96 Å respectively. The line broadening was probably due to a combination of compositional variation and lattice strain. As reported in the last quarterly progress report,[2] an x-ray fluorescence analysis of the residue extracted from the cast material indicated that its metallic composition was approximately 95% tantalum and 5% tungsten. No hafnium or rhenium was observed.

TABLE 2. Mechanical Properties of Composition NASV-20[a]
(Ta-8W-1Re-0.7Hf-0.025C)

Test Temperature (°F)	Remarks	0.2% Yield Strength (psi)	Ultimate Tensile Strength (psi)	% Elongation		% Reduction in Area
				Uniform	Total	
-320	b,d	147,700	165,300	22.0	26.3	41.9
-150	b,d	111,000	130,300	20.0	28.4	46.3
RT	b,d	85,000	105,400	16.9	25.9	49.9
RT	c,d	85,300	103,500	15.5	26.6	48.4
RT	c,e	82,800	104,600	16.3	27.5	49.3
+600	b,d	53,700	75,500	15.3	24.4	47.9
+2400	c,d	30,400	40,900		35.0	

(a) Sheet material annealed for 1 hour at 1650°C/3000°F prior to testing.

(b) Material processed from side forging.

(c) Material processed from upset forging.

(d) Strain rate 0.05 in./in./min. throughout test.

(e) Strain rate 0.005 in./in./min. through 0.6% yield and then 0.05 in./in./min for balance of test.

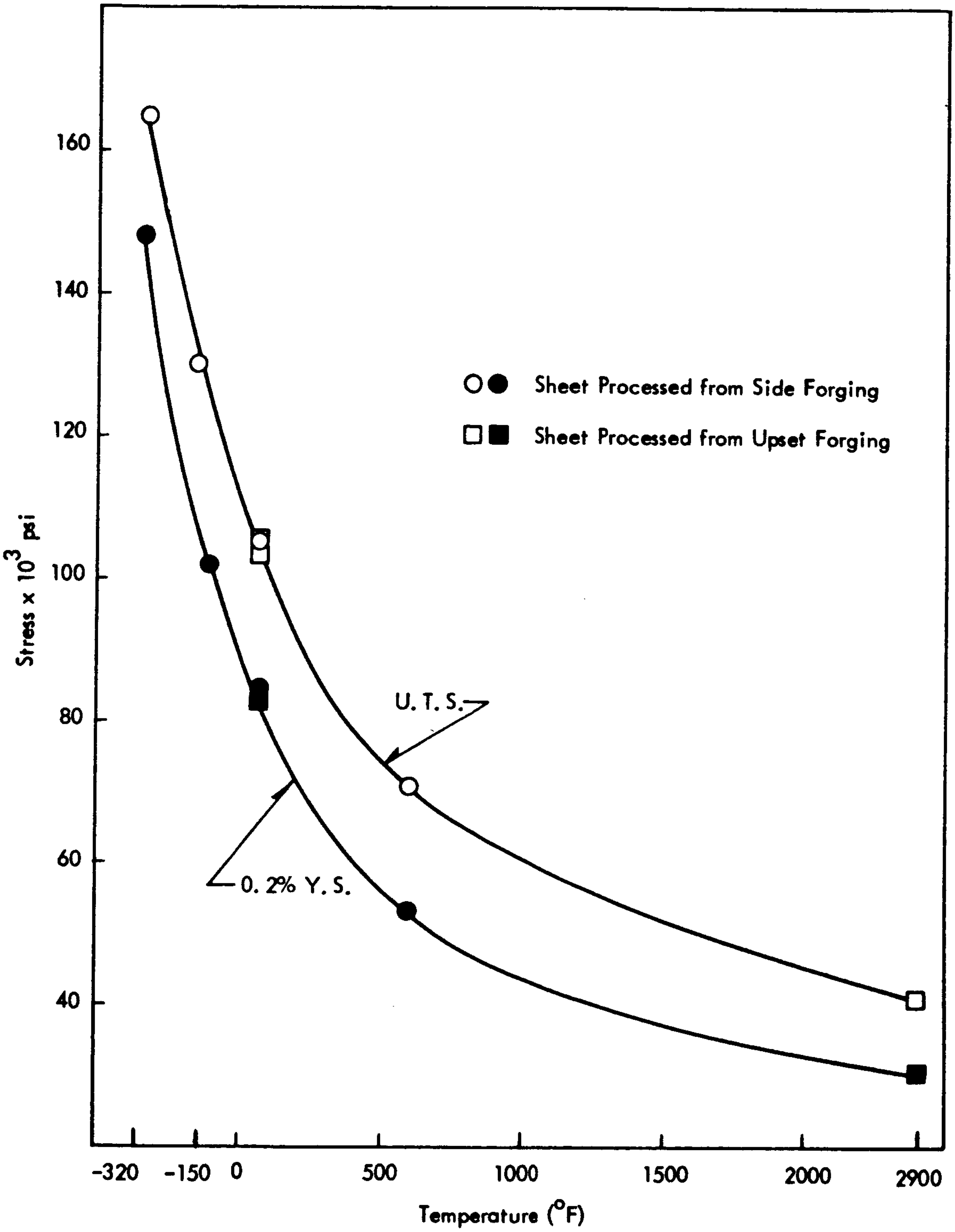

FIGURE 6 - Tensile Properties of Composition NASV-20 (Ta-8W-1Re-0.7Hf-0.025C)

Although similar analyses were not performed on the other residues there is no apparent reason to expect an appreciable difference from the above reported values. Thus, the HCP dimetal carbide phase in NASV-20 is still assumed to be accurately represented as $(Ta,W)_2C_{1-x}$.

The dimetal carbide from the as-cast NASV-20 material was studied by means of transmission electron microscopy (redispersed residue, extraction replica, and selected area electron diffraction techniques), while the bulk as-cast material was studied by means of standard 2-stage carbon surface replicas. This work indicated that the dimetal carbide consisted mostly of the flower-shaped platelets shown in Figures 7a and 7b. These platelets ranged in size from about 0.05μ to about 5μ. As the larger platelets were essentially non-transparent to the electron beam, even at 100 Kv, their thickness must exceed 2000 Å. Because of the thickness of the platelets, satisfactory selected area electron diffraction patterns could not be obtained. However, the patterns were sufficient to indicate the presence of twins and of appreciable strain and/or variable composition. The dimetal carbide was also observed in the form of very small polyhedra, 0.05 to 0.1μ (Figure 7c).

The dimetal residue extracted from the side forged material was also studied by transmission electron microscopy because of differences observed in the microstructure of the as-cast material (Figure 3) and the side-forged material (Figure 5). The general appearance of the precipitates is illustrated in Figure 8. Again the dimetal carbide was present in the form of thin platelets. However, the platelets were consistently smaller than those observed in the as-cast material (i.e., up to about 0.5μ versus up to about 5μ). Figure 8 clearly illustrates the structure of these platelets, and explains the extra "twinned" reflections observed in many of the diffraction patterns of the platelets from the as-cast material. The dimetal carbide was also observed in the form of very irregular, semi-transparent precipitates (Figure 8). These precipitates are similar to those previously found in two creep specimens of composition NAS-56 (a non-consumable arc melted button having the same composition as NASV-20), which had been annealed to 1650°C (3000°F) and tested at 1315°C (2400°F). None of the polyhedra observed in the residue extracted from the as-cast material were observed in the residue extracted from the side forged material.

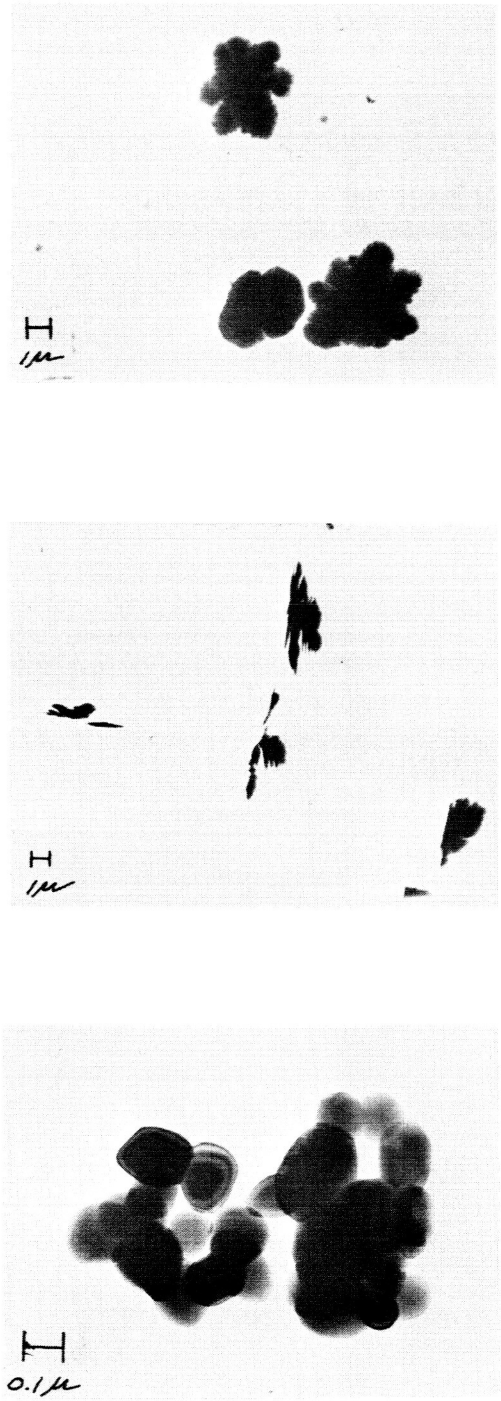

(a) Extracted Residue-Platelets
3000X

(b) Extraction Replica-Platelets
2500X

(c) Extracted Residue-Polyhedra
50,000X

FIGURE 7 - Transmission Electron Micrographs of HCP Tantalum Dimetal Carbide $(Ta,W)_2C_{1-x}$ Precipitates Extracted from Cast NASV-20 (Ta-8W-1Re-0.7Hf-0.025C)

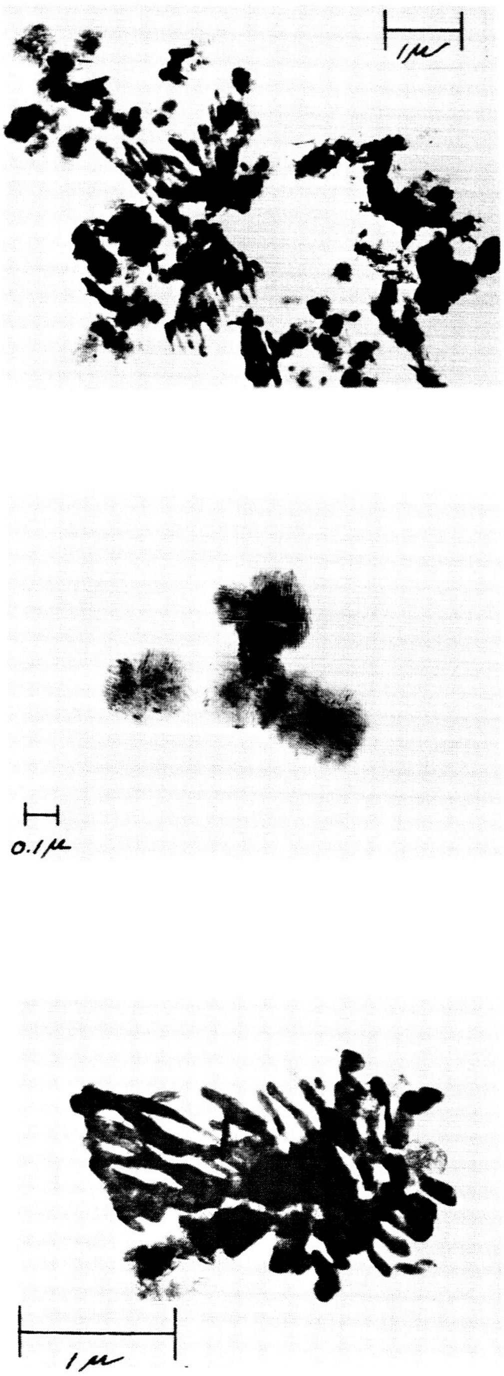

(a) 10,000X

(b) 40,000X

(c) 20,000X

FIGURE 8 - Transmission Electron Micrographs of HCP Tantalum Dimetal Carbide Precipitates Extracted from Side Forged NASV-20 (Ta-8W-1Re-0.7Hf-0.025C)

The precipitates extracted from the side forged material and shown in Figure 8 appear to have been formed during the slow cool down of the side forged ingot. This fact, if true, would indicate that the HCP tantalum dimetal carbide phase has higher solubility in NASV-20 at 1400°C (2550°F) than anticipated. Further work will be performed to determine the solubility of the dimetal carbide in NASV-20 as a function of temperature. Further work will also be performed to determine the morphology of the dimetal carbide in 0.04-inch NASV-20 sheet as a function of heat treating temperature and cooling rate.

B. OPTIMIZATION INVESTIGATION

Weldability — Extruded sheet bars of compositions NASV-16 (Ta-9.5W-0.5Re-0.25Zr-0.02C-0.01N) and NASV-17 (Ta-4W-3Re-0.75Hf-0.01C-0.02N) were processed to 0.04-inch sheet by the standard process and the ductile-brittle transition temperature of the base metal and TIG welded materials was re-evaluated. In each case the sheet was annealed for 1 hour at 1650°C (3000°F) prior to welding and/or testing. The test results are recorded in Table 3, along with the previously reported data for these two compositions. The ductile-brittle transition temperature of both base metals was slightly lower than previously reported (i.e., -250°F/-157°C versus -200°F/-129°C for NASV-16 and -250°F/-157°C versus -225°F/-143°C for NASV-17). In the case of the TIG welded NASV-16 material the DBTT was +25°F (-4°C), which is not inconsistent with the initial test data, which previously defined the transition temperature as being between +75°F (+24°C) and -25°F (-32°C). The transition temperature of the TIG welded NASV-17 material was 50°F (28°C) higher than that previously reported. The minor differences in all these redetermined transition temperatures probably reflect normal scatter due to intrinsic variations in the material composition, welding parameters, and testing conditions.

This additional data for NASV-16 and the range of transition temperature for NASV-17, in the as-TIG welded condition, are included in Figure 9, a revised plot of the effect of

TABLE 3. Ductile-Brittle Transition Temperatures of Compositions NASV-16[(a)] and NASV-17[(a)]

Composition and Heat Number	Condition	Run	Temperature °F	Temperature °C	No. Load Bend Angle (degrees)	Remarks
Ta-9.5W-0.5Re-0.25Zr-0.02C-0.01N (NASV-16)	Base Metal	1st	-200	-129	91	Bend
			-225	-143	40	Break
		2nd	-250	-157	96	Bend
			-250	-157	61	Break
	TIG Welded	1st	+75	+24	96	Bend[(b)]
			-25	-32	46	Break
		2nd	+25	-4	99	Bend[(c)]
			0	-18	64	Break
Ta-4W-3Re-0.75Hf-0.01C-0.02N (NASV-17)	Base Metal	1st	-225	-143	94	Bend
			-250	-157	40	Break
		2nd	-250	-157	90	Bend
			-250	-157	50	Break
	TIG Welded	1st	+75	+24	96	Bend[(c)]
			-25	-32	20	Break
		2nd	+125	+52	99	Bend
			+100	+38	99	Break

(a) Sheet processed from extruded ingot and annealed for 1 hour at 1650°C/3000°F prior to welding. Bend radii - 1.8t.
(b) Sample exhibited base metal failure.
(c) Sample exhibited ductile failure within weld and heat effected zone.

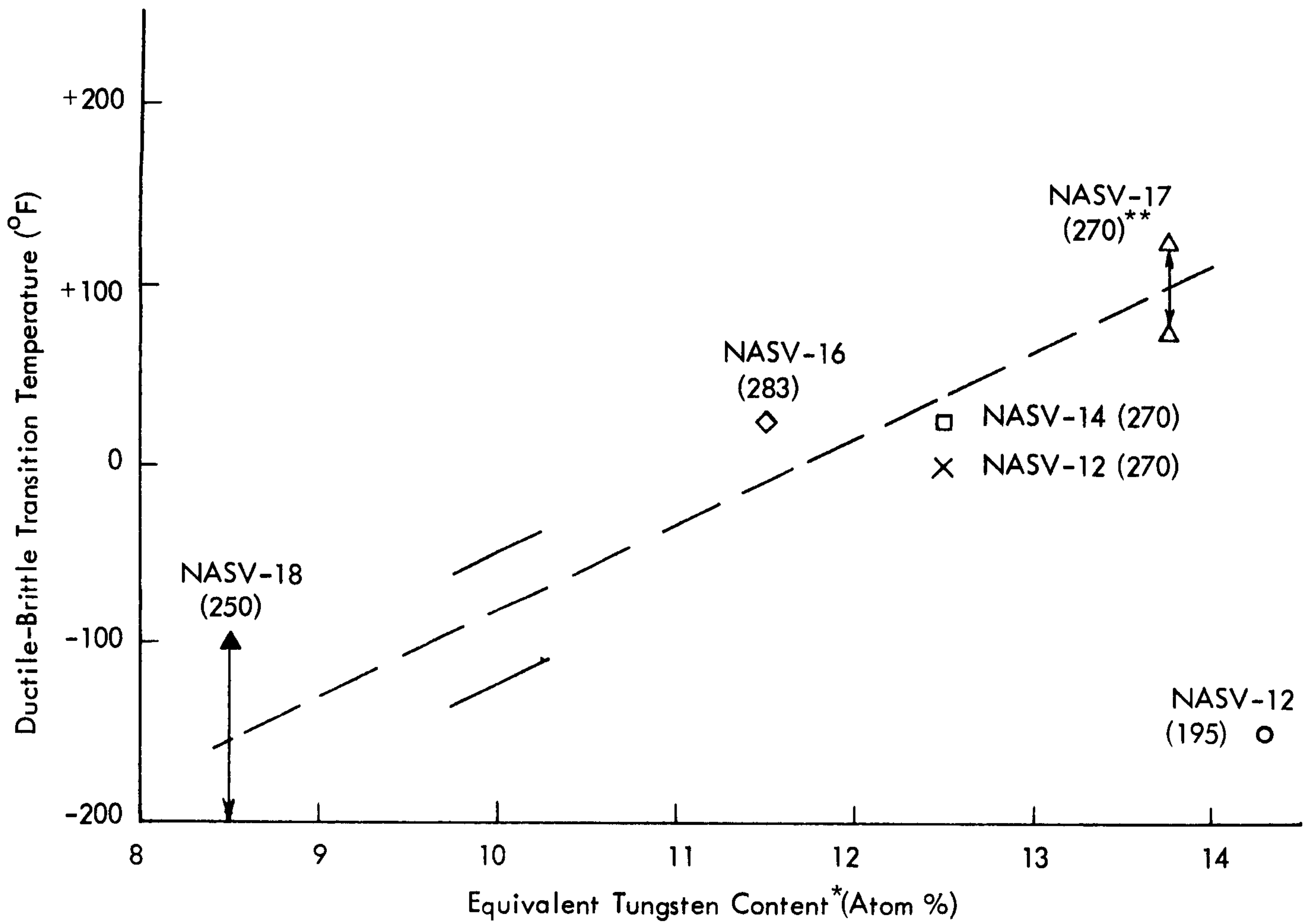

FIGURE 9 - Effect of Equivalent Tungsten Content on the Ductile-Brittle Transition Temperature of TIG Welded Optimization Compositions

*(T_E = %W + % Mo + % Hf + % Zr + 3 x % Re)

**Analyzed C+N, ppm

total equivalent tungsten content* on the ductile-brittle transition temperature of the optimization alloys.

Creep Properties — Creep tests on the remaining specimens from the optimization investigation were completed and the data obtained are reported in Table 4 and Figure 10. Specimen NASV-18E 1-C which had been initially tested at 2400°F (1315°C) and 15,000 psi elongated 1% in 67 hours, which is essentially equivalent to T-222 tested under the same conditions. After the equipment relocation was completed, this specimen was re-inserted and tested at increasingly lower temperatures. These data are in Table 5 and the resulting creep curve is shown in Figure 11. The characteristic increasing creep rate with time is evident at the upper three test temperatures. However, when the test temperature was decreased to 1987°F, the creep rate was reduced to zero. The apparent activation energy (ΔH) for creep was calculated using the relationship $\dot{\epsilon} = Ae^{-\Delta H/RT}$ where A is a constant, $\dot{\epsilon}$ is the creep rate, R is the gas constant, and T is the test temperature. Using the creep rate just preceding and following the temperature change, the following values for the activation energy were obtained.

T_1 (°F)	T_2 (°F)	$\dot{\epsilon}_1$ (%/hr.)	$\dot{\epsilon}_2$ (%/hr.)	ΔH k cal/mole
2400	2350	0.0374	0.0268	58,300
2350	2257	0.04	0.014	95,200
2257	1987	0.0272	0	∞

The activation energy for self diffusion of tantalum has been reported to be 110,000 cal/mole.[5] The activation energy for creep at test temperatures above approximately $1/2T_m$** corresponds to the activation energy for self diffusion[6] and it has been postulated that the rate controlling mechanism is one of dislocation climb.[7] The range of test temperature for NASV-18E-1C was 0.42 to 0.48 T_m. The apparent activation energy (ΔH) increased with

* Total tungsten equivalent content (a/o is derived from binary room temperature hardness data which show that for 1 a/o addition to tantalum, 1 a/o Re is three times more effective in increasing R.T. hardness than 1 a/o W, while Mo, Hf, and Zr are essentially the same as W.

** T_m (Melting Temperature)

TABLE 4 - Creep Properties of Compositions NASV-17 and NASV-18 at 1 x 10^{-8} Torr

Composition and Heat No.[b]	Test Temperature (°F)	Test Temperature (°C)	Stress (psi)	Test Time (hrs.)	Elongation (%)	Time to 1% Strain	Specimen Hardness, (DPH) Pre-Test	Specimen Hardness, (DPH) Post-Test
Ta-4W-3Re-0.75Hf -0.01C-0.02N (NASV-17)	2400	1315	12,500	284	0.27	1,020[a]	322	266
	2575	1413	8,000	331	0.96	344[a]	323	277
Ta-5W-1Re-0.3Zr -0.025N (NASV-18)	2400	1315	12,500	241	1.22	214	277	224
	2575	1413	8,000	330	2.56	157	279	224

(a) Extrapolated

(b) Specimen annealed for one hour at 1650°C (3000°F) prior to test.

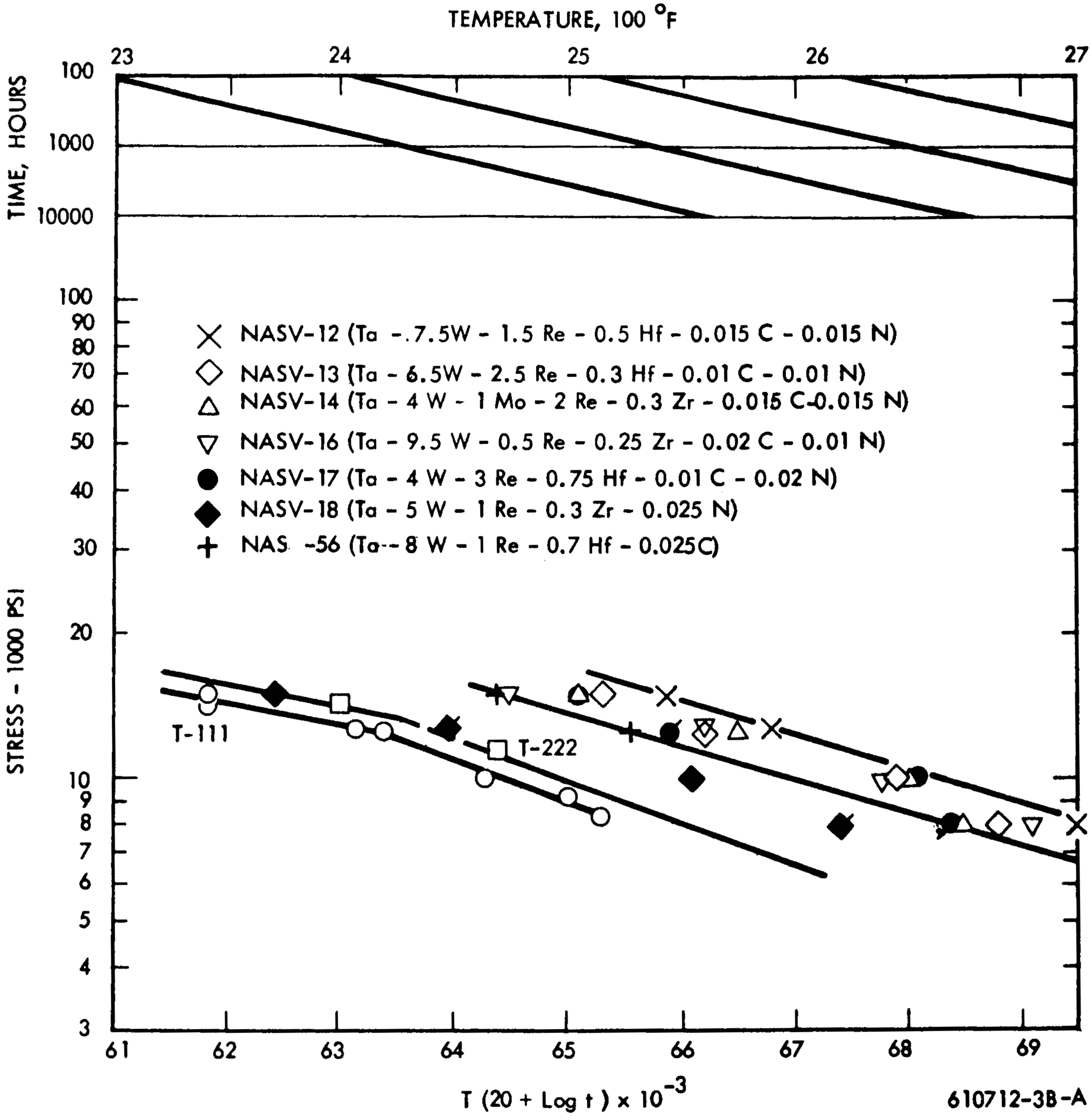

FIGURE 10 - Creep Properties of the Optimization Compositions Based on the Larson-Miller Parameter (where t = time to 1% strain in hours (all material annealed for one hour at 1650°C(3000°F) prior to test).

TABLE 5 - Temperature Change Creep Test on Composition NASV-18[b] (Ta-5W-1Re-0.3Zr-0.025N Tested at 1×10^{-8} Torr and 15,000 psi.

Test Temperature (°F)	Test Temperature (°C)	Time at Temperature (hrs.)[a]	Elongation, % Incremental	Elongation, % Cumulative	Creep Rate, % per Hr. After Temperature Change	Creep Rate, % per Hr. Preceding Temperature Change
2400	1316	93	2.12	2.12	--	0.0374
2350	1288	50 (143)	1.73	3.65	0.0268	0.040
2257	1236	260 (403)	4.98	8.58	0.0139	0.0272
1987	1086	230 (633)	0	8.41	0	--

(a) Values in parenthesis indicate total accumulated test time

(b) Specimen annealed for one hour at 1650°C (3000°F) prior to test.

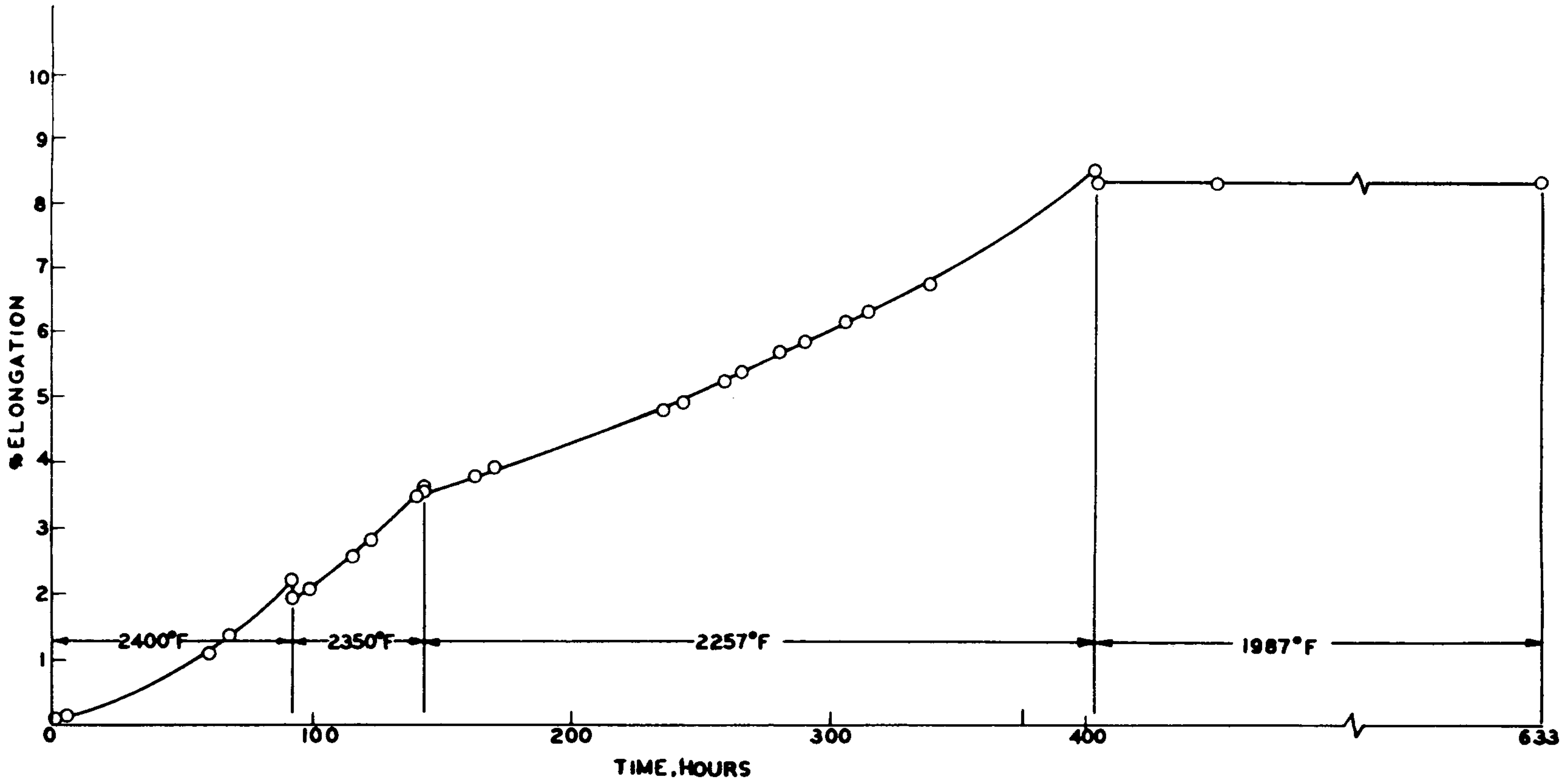

FIGURE 11 - Creep Curve for NASV-18, Temperature Change Test at a Stress of 15,000 psi. (Specimen Annealed for One Hour at 1650°C (3000°F) Prior to Test)

decreasing test temperature and the ΔH of 58,300 cal/mole measured at the highest test temperature ($0.48\,T_m$) was only about 1/2 of that of the value of ΔH for the self diffusion of tantalum indicating that a mechanism other than dislocation climb may be rate controlling. The ΔH of diffusion of nitrogen in tantalum is reported as 39,800 cal/g mole[8] and is in reasonable agreement with the value of ΔH measured at 2350-2400°F inferring possibly an interstitial-dislocation interaction rate controlling mechanism as proposed by Conrad.[9] However, it is not apparent from the values of activation energy just what the rate controlling mechanism may be. The rapid increase in ΔH over the rather narrow temperature range is similar to the effect that was observed by Dorn[10] when testing Al-Mg alloys. The reasons for these pertubations is attributable to the solute addition but the exact mechanism is not understood.[10] Also, the simplifying assumptions made in using the equation $\epsilon = Ae^{-\Delta H/RT}$ (i. e., constant structure and A is constant) may not apply to the complex alloy which most likely does not have a constant structure over the test temperature range.

C. PHASE IDENTIFICATION AND MORPHOLOGY

During the quarter, the intersection of the four-phase fields in the tantalum-rich corner of the (Ta + W)-Hf-C phase diagram (1315°C/2400°F isotherm) was more precisely defined. This intersection had been defined by a single data point (i. e., Ta-39; Ta-9.6W-2.4Hf-0.01C), hence the material was re-evaluated for its carbon content (130 ppm) and its contained phases. The contained phases, extracted from the head section of a creep specimen, which had been annealed for 1 hour at 1650°C (3000°F) and tested for 386 hours at 1315°C (2400°F) plus 114 hours at 2335°F under a stress of 14,500 psi in a vacuum of $<1 \times 10^{-8}$ torr, were identified by the standard Debye-Scherrer x-ray diffraction technique. Present were the FCC hafnium carbide phase having a lattice parameter, a_o, of 4.60 Å and a minor amount of monoclinic HfO_2. No HCP dimetal carbide was observed. These results are in conflict with the earlier results which indicated the presence of the HCP tantalum dimetal carbide as well as the FCC hafnium monocarbide. The absence of the HCP phase was further confirmed in a second specimen which had been solution heat treated for 1 hour at 1650°C (3000°F), helium quenched, and then aged for 16 hours at 1315°C (2400°F). Apparently the original sample of Ta-39 had a composition variation or some HCP phase originally precipitates from the solid solution and slowly transforms to the FCC phase. Figure 12 reflects the change in the phase diagram. The dotted lines on Figure 12 are phase boundaries for the Ta-Hf-C system as extrapolated from Rudy's data.[11]

III. FUTURE WORK

During the next quarterly period it is planned to accomplish the following:

1. Complete the evaluation of NASV-20 for weldability, creep resistance, and fabricability characteristics.

2. Continue phase identification and morphology studies in detail on NASV-20.

3. Establish the composition for the second 4-inch diameter optimized composition and start assembly of the first melt electrode.

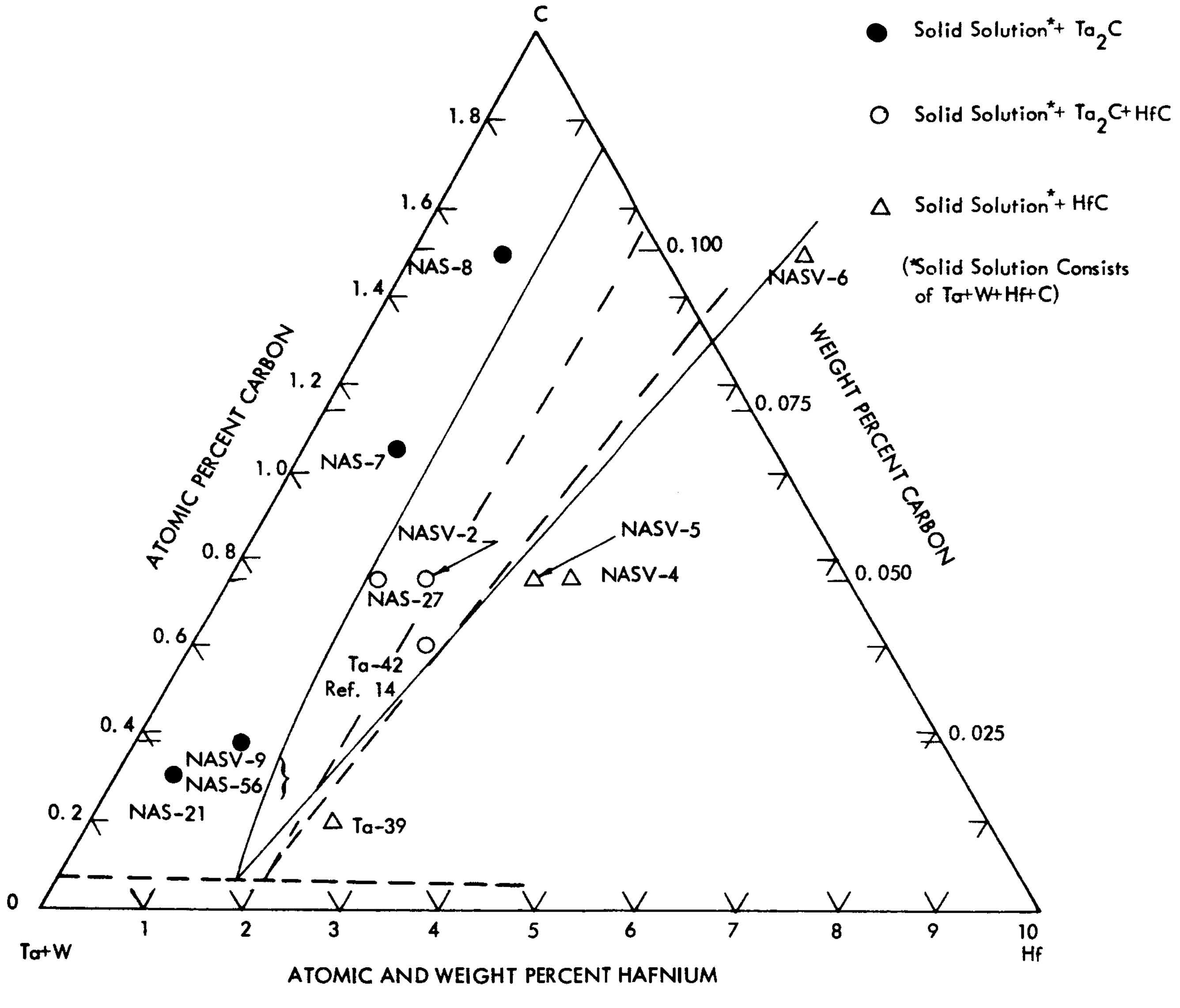

FIGURE 12 - Tantalum Rich Corner of the (Ta+W)-Hf-C Psuedo Ternary Phase Diagram (1315°C/2400°F Isotherm)

IV. REFERENCES

1. R. W. Buckman, Jr. and R. T. Begley, "Development of Dispersion Strengthened Tantalum Base Alloy", Final Technical Report, Phase I, WANL-PR-(Q)-004, to be published.

2. R. W. Buckman, Jr. and R. C. Goodspeed, "Development of Dispersion Strengthened Tantalum Base Alloy", Seventh Quarterly Report, WANL-PR-(Q)-008, NASA-CR-54894.

3. R. W. Buckman, Jr. and R. C. Goodspeed, "Development of Dispersion Strengthened Tantalum Base Alloy", Sixth Quarterly Report, WANL-PR-(Q)-007, NASA-CR-54658

4. R. T. Begley, W. N. Platte, R. L. Ammon, and A. I. Lewis, "Development of Niobium Base Alloys", WADC-TR-57-344, Part V, January 1961.

5. R. Resnick and L. S. Castleman, Trans. AIME, p. 218, 307, 1960.

6. F. Garafalo, Fundamentals of Creep and Creep-Rupture in Metals, p. 87, Macmillan Series in Materials Science, 1965.

7. J. Weertman, "Theory of Steady State Creep Based on Dislocation Climb", Journal of Applied Physics, Vol. 26, No. 10, p. 1213, 1955.

8. C. Y. Ang, "Activation Energies and Diffusion Coefficients of Oxygen and Nitrogen in Niobium and Tantalum", Acta Met. 1, p. 123, 1953.

9. H. Conrad, "Thermally Activated Deformation of Metals", Journal of Metals, Vol. 16,7, p. 587, 1964.

10. J. E. Dorn, "A Survey of Recent Results on Experimental Determinations of Activation Energies for Creep", Presented at Fourth Sagamore Ordnance Materials Research Conference, Racquette Lake, New York, August 21-23, 1957.

11. E. Rudy and H. Nowotony, Untersuchen in System Hafnium-Tantalum-Kohlenstaff, Mh. Chemie, 94, p. 507-517, 1963.

APPENDIX I

Compositions of alloys discussed in this report are listed below:

Consumable Electrode Melted (2 Inch Diameter Ingots)

Heat Number	Composition Weight Percent
NASV-2	Ta-8W-2Hf-0.05C
NASV-4	Ta-8W-2.7Hf-0.4Zr-0.05C
NASV-5	Ta-9.6W-3.15Hf-0.05C
NASV-6	Ta-9.6W-3.90Hf-0.10C
NASV-7	Ta-5.7W-1.56Re-0.7Mo-0.25Hf-0.13Zr -0.015N-0.015C
NASV-8	Ta-5.7W-1.56Re-0.7Mo-0.75Hf-0.13Zr -0.015N-0.015C
NASV-9	Ta-9W-1Hf-0.025C
NASV-10	Ta-7.1W-1.56Re-0.25Hf-0.12Zr-0.03N
NASV-11	Ta-9W-1.5Re-1Hf-0.015C-0.015N
NASV-12	Ta-7.5W-1.5Re-0.5Hf-0.015C-0.015N
NASV-13	Ta-6.5W-2.5Re-0.3Hf-0.01C-0.01N
NASV-14	Ta-4W-1Mo-2Re-0.3Zr-0.015C-0.015N
NASV-15	Ta-9W-1.5Re-1Hf-0.06N
NASV-16	Ta-9.5W-0.5Re-0.25Zr-0.02C-0.01N
NASV-17	Ta-4W-3Re-0.75Hf-0.01C-0.02N
NASV-18	Ta-5W-1Re-0.3Zr-0.025N
T-333 (NASV-20)*	Ta-8W-1Re-0.7Hf-0.025C

Non-Consumable Electrode Melted (800 Gram Ingots)

NAS-7	Ta-8.2W-1Hf-0.07C
NAS-8	Ta-8.2W-1Hf-0.10C
NAS-21	Ta-8.6W-0.53Hf-0.02C
NAS-27	Ta-4.6W-1.5Hf-0.05C
NAS-36	Ta-5.7W-1.56Re-0.7Mo-0.25Hf-0.13Zr -0.015C-0.015N
NAS-56-57	Ta-8W-1Re-0.7Hf-0.025C

*4 Inch Diameter Ingot.

APPENDIX II

NASV-20 (Ta-8W-1Re-0.7Hf-0.025C)

As upset forged.

Intensity	d	Phase
MW	2.70	HCP
MW	2.48	HCP
S	2.37	HCP
M	2.33	BCC
W	1.825	HCP
VW	1.65	BCC
W	1.555	HCP
W	1.410	HCP
W	1.350	HCP, BCC
W	1.320	HCP
W	1.300	HCP
W	1.040	HCP, BCC
VW	0.998	HCP
VVW	0.970	HCP
VW	0.882	BCC
VW	0.868	HCP

NOTE:

HCP phase assumed to be $(Ta,W)_2C_{1-x}$ (diffraction lines are too weak and not well enough resolved to accurately determine lattice parameters).

BCC a_o = 3.30Å assumed to be Ta.

NASV-20 (Ta-8W-1Re-0.7Hf-0.025C)

0.04-Inch sheet processed from upset forging (in as-rolled condition)

Intensity	d	Phase
M	2.68	HCP
M	2.47	HCP
VS	2.36	HCP
VS	2.33	BCC
M	1.815	HCP
MW	1.65	BCC
M	1.55	HCP
M	1.405	HCP
M	1.345	HCP, BCC
M	1.315	HCP
MW	1.295	HCP
VVW	1.230	HCP
VW	1.180	HCP
VW	1.165	BCC
MW	1.040	BCC
MW	0.995	HCP
VW	0.965	HCP
M	0.880	BCC
VW	0.864	HCP

NOTE: HCP phase assumed to be $(Ta,W)_2C_{1-x}$ (diffraction lines are too weak and not well enough resolved to accurately determine lattice parameters).
BCC a_o = 3.30Å assumed to be Ta.

NASV-20 (Ta-8W-1Re-0.7Hf-0.025C)

As side forged.

Intensity	d	Phase
M	2.70	HCP
M	2.48	HCP
S	2.37	HCP
S	2.34	BCC
M	1.825	HCP
M	1.65	BCC
M	1.56	HCP
M	1.41	HCP
M	1.348	HCP, BCC
MW	1.320	HCP
MW	1.300	HCP
VW	1.240	HCP
VVW	1.182	HCP
MW	1.168	BCC
M	1.043	HCP, BCC
MW	0.998	HCP
W	0.970	HCP
VW	0.952	BCC
VVW	0.944	HCP
VW	0.930	HCP
M	0.882	BCC
W	0.868	HCP
VW	0.844	HCP

NOTE: HCP phase assumed to be $(Ta,W)_2C_{1-x}$ (diffraction lines are too weak and not well enough resolved to accurately determine lattice parameters). BCC $a_o = 3.30\mathring{A}$ assumed to be Ta.

NASV-20 (Ta-8W-1Re-0.7Hf-0.025C)

0.06-inch sheet processed from side forging (in as-rolled condition)

Intensity	d	Phase
M	2.70	HCP
M	2.47	HCP
S	2.36	HCP
MS	2.34	BCC
M	1.82	HCP
MW	1.65	BCC
M	1.555	HCP
M	1.405	HCP
M	1.349	HCP, BCC
MW	1.318	HCP
MW	1.295	HCP
VVW	1.180	HCP
VW	1.165	BCC
VVW	1.125	HCP
M	1.043	BCC
MW	0.995	HCP
VW	0.968	HCP
VVW	0.940	HCP

NOTE:

HCP phase assumed to be $(Ta,W)_2C_{1-x}$ (diffraction lines are too weak and not well enough resolved to accurately determine lattice parameters).

BCC $a_o = 3.30\mathring{A}$ assumed to be Ta.

T-222 (Ta-9.6W-2.4Hf-0.01C)

Creep specimen (Ta-39-1)-gage length

Intensity	d	Phase
VW	3.15	HfO_2
VW	2.93	β(2.65)
VW	2.82	HfO_2
VS	2.65	FCC
VVW	2.54	β(2.29)
VVW	2.32	BCC
VS	2.29	FCC
VVW	1.80	β(1.625)
S	1.625	FCC
VVW	1.535	β(1.365)
S	1.385	FCC
VVW	1.345	BCC
M	1.326	FCC
W	1.150	FCC
M	1.055	FCC
M	1.029	FCC
M	0.940	FCC
M	0.886	FCC
M	0.824	FCC
S	0.7775	FCC

NOTE: FCC $a_o = 4.60Å$ assumed to be $(Hf,Ta)C_{1-x}$

BCC $a_o = 3.30Å$ assumed to be Ta

T-222 (Ta-9.6W-2.4Hf-0.01C)

Creep specimen (Ta-39-1)-head section

Intensity	d	Phase
VW	2.94	β(2.65)
VS	2.65	FCC
VW	2.55	β(2.29)
M	2.34	BCC
VS	2.29	FCC
VW	1.80	β(1.625)
W	1.650	BCC
S	1.625	FCC
VVW	1.54	β(1.389)
S	1.387	FCC
M	1.345	BCC
M	1.328	FCC
VW	1.167	BCC
MW	1.152	FCC
M	1.057	FCC
VW	1.042	BCC
M	1.030	FCC
VW	0.950	BCC
M	0.940	FCC
M	0.887	FCC
VW	0.881	BCC
MW	0.814	FCC
S	0.778	FCC

NOTE: FCC $a_o = 4.61Å$ assumed to be $(Hf,Ta)C_{1-x}$

BCC $a_o = 3.30Å$ assumed to be Ta

DISTRIBUTION LIST

TRW
Caldwell Research Center
23555 Euclid Avenue
Cleveland, Ohio 44117
Attn: Librarian
Attn: G. J. Guarnieri

TRW
New Devices Laboratories
7209 Platt Avenue
Cleveland, Ohio 44104
Attn: Librarian

National Aeronautics and Space Adm.
Washington, D. C. 20546
Attn: Walter C. Scott
Attn: James J. Lynch (RN)
Attn: George C. Deutsch (RR)

National Aeronautics and Space Adm.
Scientific and Technical Inf. Facility
Box 5700
Bethesda, Maryland 21811

National Aeronautics and Space Adm.
Ames Research Center
Moffet Field, California 94035
Attn: Librarian

National Aeronautics and Space Adm.
Goddard Space Flight Center
Greenbelt, Maryland 20771
Attn: Librarian

National Aeronautics and Space Adm.
Langley Research Center
Hampton, Virginia 23365
Attn: Librarian

National Aeronautics and Space Adm.
Manned Spacecraft Center
Houston, Texas 77001
Attn: Librarian

National Aeronautics and Space Adm.
George C. Marshall Space Flight Center
Huntsville, Alabama 35812
Attn: Librarian
Attn: Wm. A. Wilson

National Aeronautics and Space Adm.
Jet Propulsion Laboratory
4800 Oak Grove Drive
Pasadena, California 91103
Attn: Librarian

National Aeronautics and Space Adm.
21000 Brookpark Road
Cleveland, Ohio 44135
Attn: Librarian
Attn: Dr. Bernard Lubarsky
Attn: Mr. Roger Mather
Attn: Mr. G. M. Ault
Attn: Mr. J. Joyce
Attn: Mr. P. E. Moorhead
Attn: Mr. N. T. Musial
Attn: Mr. T. Strom
Attn: Mr. T. A. Moss
Attn: Dr. Louis Rosenblum
Attn: J. Creagh
Attn: Mr. J. Dilley
Attn: Mr. G. K. Watson
Attn: Mr. T. Moore
Attn: Mr. G. Tulsiak
Attn: NASA-Lewis Laboratory Report Central Section

National Aeronautics and Space Adm.
Western Operations Office
150 Pico Boulevard
Santa Monica, California 90406
Attn: Mr. John Keeler

National Bureau of Standards
Washington 25, D. C.
Attn: Librarian

Aeronautical Systems Division
Wright-Patterson Air Force Base, Ohio
Attn: Charles Armbruster
Attn: T. Cooper
Attn: Librarian
Attn: John L. Morris
Attn: H. J. Middendorp

Army Ordnance Frankford Arsenal
Bridesburg Station
Philadelphia 37, Pennsylvania
Attn: Librarian

Bureau of Ships
Dept. of the Navy
Washington 25, D. C.
Attn: Librarian

Bureau of Weapons
Research and Engineering
Material Division
Washington 25, D. C.
Attn: Librarian

U. S. Atomic Energy Commission
Technical Reports Library
Washington 25, D. C.
Attn: J. M. O' Leary

U. S. Atomic Energy Commission
Germantown, Maryland
Attn: Col. E. L. Douthett
Attn: H. Rochen
Attn: Major Gordon Dicker

U. S. Atomic Energy Commission
Technical Information Service Extension
P. O. Box 62
Oak Ridge, Tennessee

U. S. Atomic Energy Commission
Washington 25, C. C.
Attn: M. J. Whitman

Argonne National Laboratory
9700 South Cross Avenue
Argonne, Illinois
Attn: Librarian

Brookhaven National Laboratory
Upton, Long Island, New York
Attn: Librarian

Oak Ridge National Laboratory
Oak Ridge, Tennessee
Attn: W. O. Harms
Attn: Dr. A. J. Miller
Attn: Librarian
Attn: N. T. Bray

Office of Naval Research
Power Division
Washington 25, D. C.
Attn: Librarian

U. S. Naval Research Laboratory
Washington 25, D. C.
Attn: Librarian

Advanced Technology Laboratories
Division of American Standard
369 Whisman Road
Mountain View, California
Attn: Librarian

Aerojet General Corporation
P. O. Box 296
Azusa, California
Attn: Librarian

Aerojet General Nucleonics
P. O. Box 77
San Ramon, California
Attn: Librarian

AiResearch Manufacturing Company
Sky Harbor Airport
402 South 36th Street
Phoenix, Arizona
Attn: Librarian
Attn: E. A. Kovacevich

AiResearch Manufacturing Company
9851-9951 Sepulveda Boulevard
Los Angeles 45, California
Attn: Librarian

I. I. T. Research Institute
10 W. 35th Street
Chicago, Illinois 60616

Atomics International
8900 DeSoto Avenue
Canoga Park, California

Avco
Research and Advanced Development Dept.
201 Lowell Street
Wilmington, Massachusetts
Attn: Librarian

Babcock and Wilcox Company
Research Center
Alliance, Ohio
Attn: Librarian

Battelle Memorial Institute
505 King Avenue
Columbus, Ohio
Attn: C. M. Allen
Attn: Librarian
Attn: Defense Metals Inf. Center

The Bendix Corporation
Research Laboratories Div.
Southfield, Detroit 1, Michigan
Attn: Librarian

Bell Aerosystems Co.
P. O. Box 1
Buffalo 5, New York
Attn: E. J. King

The Boeing Company
Seattle, Washington
Attn: Librarian

Brush Beryllium Company
17876 St. Clair Avenue
Cleveland, Ohio 44110
Attn: Librarian

Carborundum Company
Niagara Falls, New York
Attn: Librarian

Chance Vought Aircraft Inc.
P. O. Box 5907
Dallas 22, Texas
Attn: Librarian

Clevite Corporation
Mechanical Research Division
540 East 105th Street
Cleveland 8, Ohio
Attn: Mr. N. C. Beerli

Climax Molybdenum Company of Michigan
1600 Huron Parkway
Ann Arbor, Michigan
Attn: Librarian

Convair Astronautics
50001 Kerrny Villa Road
San Diego 11, California
Attn: Librarian

E. I. duPont deNemours and Co. , Inc.
Wilmington 98, Delaware
Attn: Librarian

Electro-Optical Systems, Inc.
Advanced Power Systems Division
Pasadena, California
Attn: Librarian

Fansteel Metallurgical, Corp.
North Chicago, Illinois
Attn: Librarian

Ford Motor Company
Aeronutronics
Newport Beach, California
Attn: Librarian

General Dynamics/General Atomic
P. O. Box 608
San Diego, California 92112
Attn: Librarian

General Electric Company
Atomic Power Equipment Div.
P. O. Box 1131
San Jose, California

General Electric Company
Flight Propulsion Laboratory Dept.
Cincinnati 15, Ohio
Attn: Librarian
Attn: Dr. J.W. Semmel

General Electric Company
Missile and Space Vehicle Dept.
3198 Chestnut Street
Philadelphia 4, Pennsylvania
Attn: Librarian

General Electric Company
Vallecitos
Vallecitos Atomic Lab.
Pleasanton, California
Attn: Librarian

Herring Corp.
7356 Greenback Drive
Hollywood, California 91605
Attn: Don Adams

General Dynamics/Fort Worth
P. O. Box 748
Fort Worth, Texas
Attn: Librarian

General Motors Corporation
Allison Division
Indianapolis 6, Indiana
Attn: Librarian

Hamilton Standard
Div. of United Aircraft Corp.
Windsor Locks, Connecticut
Attn: Librarian

Hughs Aircraft Company
Engineering Division
Culver City, California
Attn: Librarian

Lockheed Missiles and Space Div.
Lockheed Aircraft Corp.
Sunnyvale, California
Attn: Librarian

Marquardt Aircraft Co.
P. O. Box 2013
Van Nuys, California
Attn: Librarian

The Martin Company
Baltimore 3, Maryland
Attn: Librarian

The Martin Company
Nuclear Division
P. O. Box 5042
Baltimore 20, Maryland
Attn: Librarian

Martin Marietta Corp.
Metals Technology Laboratory
Wheeling, Illinois

Massachusetts Institute of Technology
Cambridge 39, Massachusetts
Attn: Librarian

Materials Research and Development
Manlabs Inc.
21 Erie Street
Cambridge 39, Massachusetts

Materials Research Corporation
Orangeburg, New York
Attn: Librarian

McDonnell Aircraft
St. Louis, Missouri
Attn: Librarian

MSA Research Corporation
Callery, Pennsylvania
Attn: Librarian

North American Aviation
Los Angeles Division
Los Angeles 9, California
Attn: Librarian

National Research Corp.
Metals Division
45 Industrial Place
Newton, Massachusetts 02164
Attn: Dr. M. L. Torte
Director of Metallurgical Research

Lawrence Radiation Laboratory
Livermore, California
Attn: Dr. James Hadley
Head, Reactor Division

Pratt & Whitney Aircraft
400 Main Street
East Hartford 8, Connecticut
Attn: Librarian

Republic Aviation Corporation
Farmingdale, Long Island, New York
Attn: Librarian

Solar
2200 Pacific Highway
San Diego 12, California

Southwest Research Institute
8500 Culebra Road
San Antonio 6, Texas
Attn: Librarian

Rocketdyne
Canoga Park, California
Attn: Librarian

Superior Tube Co.
Norristown, Pennsylvania
Attn: Mr. A. Bound

Sylvania Electric Products, Inc.
Chem. & Metallurgical
Towanda, Pennsylvania
Attn: Librarian

Temescal Metallurgical
Berkeley, California
Attn: Librarian

Union Carbide Stellite Corp.
Kokomo, Indiana
Attn: Librarian

Union Carbide Metals
Niagara Falls, New York
Attn: Librarian

Union Carbide Nuclear Company
P. O. Box X
Oak Ridge, Tennessee
Attn: X-10 Laboratory Records Department

United Nuclear Corporation
5 New Street
White Plains, New York
Attn: Librarian
Attn: Mr. Albert Weinstein

Astronuclear Laboratory

Universal Cyclops Steel Corp.
Refractomet Division
Bridgeville, Pennsylvania
Attn: C. P. Mueller

TRW Space Technology Laboratories
One Space Park
Redondo Beach, California
Attn: Librarian

University of California
Lawrence Radiation Lab.
P. O. Box 808
Livermore, California
Attn: Librarian

University of Michigan
Department of Chemical & Metallurgical Eng.
Ann Arbor, Michigan
Attn: Librarian

Vought Astronautics
P. O. Box 5907
Dallas 22, Texas
Attn: Librarian

Wolverine Tube Division
Calumet & Hecla, Inc.
17200 Southfield Road
Allen Park, Michigan
Attn: R. C. Cash

Wyman-Gordon Co.
North Grafton, Massachusetts
Attn: Librarian

Wah Chang Corporation
Albany, Oregon
Attn: Librarian